Analytical Cellular Pathology 14 (1997) 111–123
IOS Press

Morphological heterogeneity of p53 positive and p53 negative nuclei in breast cancers stratified by clinicopathological variables

Katrin Friedrich*, Volker Dimmer, Gunter Haroske, Wolfdietrich Meyer, Franz Theissig, Berit Thieme and Klaus Dietmar Kunze
Institute of Pathology, Medical Faculty, Technical University, Dresden, Germany

Received 17 September 1996
Revised 20 April 1997

Abstract. The study was aimed to detect differences in nuclear morphology between nuclear populations as well as between tumours with different p53 expression in breast cancers with different clinicopathological features, which also reflect the stage of tumour progression. The p53 immunohistochemistry was performed on paraffin sections from 88 tumour samples. After the cells had been localised by means of an image cytometry workstation and their immunostaining had been categorised visually, the sections were destained and stained by the Feulgen protocol. The nuclei were relocated and measured cytometrically by the workstation.

There were significant differences in the nuclear features between tumours as well as between nuclear populations with different p53 expression in the most subgroups. The variability of nuclear shape in tumour groups, classified by the tumour size or the lymph node status, increase with the p53 immunoreactive score, whereas in tumours grouped by the Bloom–Richardson grade features of the chromatin distribution were different between the p53 staining categories.

The nuclear subpopulations showed differences in the amount and distribution of chromatin in most subgroups.

The results demonstrate the relationship between the nuclear morphology and the p53 expression in different stages of breast cancers. The p53 status is an important factor of the biological behaviour but not the only one.

Keywords: Image cytometry, chromatin structure, breast cancer, p53 immunohistochemistry

1. Introduction

The p53 gene is one of the most studied tumour suppressor genes and this is also true for breast cancer. Mutations of the p53 gene may lead to a loss of the control function of the p53 wild type in the cell cycle, resulting in a higher genetic instability [23,25,27]. Consequently, the mutated p53 protein should play an important role in the malignant transformation and tumour progression. The simplest detection of the mutated p53 protein by immunohistochemistry is based on a longer life time of the mutated gene product in contrast to that of the wild type [27].

*Corresponding author. Address: University of Technology Dresden, Institute of Pathology, Fetscherstr. 74, 01307 Dresden, Germany. Tel.: +49 351 4583033; fax: +49 351 4584358.

Some studies have demonstrated correlations between the immunohistochemical evidence of the p53 and prognosticly unfavourable clinicopathological features [7–9,11,12,16,17,21,29,31,32,34]. On the other hand, some studies showed a prognostic importance of the p53 expression for subgroups of breast cancer only, i.e., for node negative tumours [1,36].

The loss of the p53 function leads to further changes of the genome, which result also in changes of the structure of the nuclei. Previously, we reported differences in the nuclear morphology in breast cancer cells with different p53 immunoreactivity by TV based cytometry. Differences could be found in the nuclear shape, in the amount, and in the statistical and topographical distribution of the chromatin [18].

Other studies also describe correlations between prognostic relevant clinicopathological features and the nuclear morphology [2,19,24,30,37,38].

In diagnostic tumour pathology the clinicopathological characteristics of a tumour are interpreted as hints for the prognosis since they may predict the process of tumour progression.

The present study was aimed at detecting morphological differences in correlation to the p53 expression in subgroups of breast cancer with special clinicopathological characteristics, i.e., tumour size, nodal status or histological grade of malignancy. In detail, we wanted to know, whether the p53 expression in those subgroups is associated with a specific nuclear pattern. Finally, the question should be answered whether morphologic differences in those subgroups are associated with morphological differences of the nuclear image in distinct p53 subpopulations.

2. Material and methods

The study included tissue samples from 49 p53 positive and 39 p53 negative breast cancers. The cases were selected in order to find a large number of p53 positive cancers. The tumours were classified according to the nomenclature of the WHO [22]. The histological grade of malignancy was determined according to the criteria of Scarff, Bloom and Richardson [6]. The clinicopathological data are listed in Table 1.

Table 1
Clinical data

	p53 positive cases	p53 negative cases
Tumour size		
pT1	20	18
pT2	27	18
pT3	1	1
pT4	1	1
pTx	0	1
Lymph node status		
pN0	23	19
pN1	20	17
pN2	1	0
pNx	5	3
Bloom–Richardson grading		
G1	3	8
G2	18	19
G3	28	12
Age	58.5 (range 27–87)	59 (range 36–83)

The immunohistochemical detection of p53 protein was done employing dewaxed paraffin sections of routinely fixed tissue samples. The mean time of fixation in unbuffered formalin was 24 hr. After a microwave pre-treatment the sections were stained with the monoclonal antibody DO-1 (original supernatant [39], 1 : 50 dilution, incubation for 24 hr at 4 °C) in an ABC system. The chromogen was 3-amino-9-ethylcarbazol (AEC). Haemalaun was used for the counterstaining of nuclei. Finally, the sections were embedded in glycerol gelatine. The result of the immunostaining was expressed as an immunoreactive score, which takes into account the percentage of positive cells as well as the staining intensity [35]. The score ranges from 0 (negative) to 12 (maximum positive reaction). Tumours with a score equal or higher than 1 were regarded as p53 positive.

After immunostaining in each case, 500 tumour cell nuclei were localised by means of a high resolution image cytometry workstation (see Table 2). In the same step, the staining intensity of each nucleus was categorised subjectively in four categories (negative, weakly, moderately and strongly positive).

After destaining during a 45 min 5N HCl hydrolysis at room temperature the sections were Feulgen stained with pararosanilin Schiff's reagent for 60 min. The actual section thickness was measured by means of the confocal laser scanning microscope LSM-10 (Zeiss, Germany) at three different sites per section, in order to correct the cut effects on the integrated optical density related features [18]. The previously coded nuclei were relocated and measured by means of the high resolution image cytometry workstation consisting of an Axioplan microscope (Zeiss, Germany) equipped with a 486/66 MHz IBM compatible PC with a MFG frame grabber (Imaging Technology, USA) using a CCD TV camera XC-77 CE (Sony, Japan). The microscope was coupled to a computer controlled motor driven xy-scanning stage for relocation of nuclei. The software is based on the OPTIMAS image analysis system (OPTIMAS corporation, Seattle, WA, USA) and also includes correction procedures for section thickness, diffraction and glare [20] (Table 2).

Ninety-seven nuclear features from each nucleus derived from the segmented extinction image were computed by a MicroVAX 4000 computer (DEC, Maynard, MA, USA) which is connected via Ethernet to the image analysis workstation. The features describe the size and shape of the nucleus, the amount, the statistical and topographical distribution of the chromatin and the chromatin statistics of the "flat image". The nuclei appeared colourless after the destaining of the immunostaining. Nevertheless, features that may be affected due to the foregoing immunohistochemistry and which could not be

Table 2
Technical equipment for the image cytometry system

Instrument	Specification	Source
Microscope	Axioplan®	Zeiss
Light source	Halogen lamp 12 V/100 W	Zeiss
Power supply	not specified	Zeiss
Filter	Green filter 570 nm	Zeiss
Condensor	Condensor 0.9	Zeiss
Objective	Plan NEOFLUAR × 63/1.25 oil	Zeiss
xy-scanning stage	with MCU 26	Zeiss
Adapter	C-mount without optical lenses	Zeiss
TV camera	XC77CE pixel size: 11 × 11 μm; 0.03 μm^2 in the object plane	Sony
Frame grabber	MFG	Imaging Technology
Image analysis basic software	Optimas®	OPTIMAS

equalised by the mean optical density were excluded from the statistical analysis. Table 3 shows a short description of the cytometric features with statistical relevance in this study.

The purpose of this study was to detect different patterns of the nuclear morphological features in correlation to the p53 status and the clinicopathological stage. The stepwise multivariate discriminant analysis is able to find such combinations.

These analyses based on the mean values and their standard deviations of the features from the nuclear populations in each staining category in each case, were performed by means of a self written software program REDUGD. According to the Bonferroni principle, the significance level desired for the actual discrimination ($p < 0.1$) has to be divided by the appropriate degree of freedom. The degree of freedom is equal to the number of uncorrelated variables, if the number of these variables exceed the number of cases, then the number of cases corresponds with the degree of freedom. The number of tumours with a Bloom–Richardson grade 1 was too small for the statistical analysis and could not be considered in the following comparisons.

The procedure of analysis is summarised in a flow chart in Table 4.

Table 3
Selection of the cytometric features (with statistical relevance in this study)

Acronym	Short description
FormFak	Shape factor of the nucleus
RVKonv	Radius of the nuclear convex contour
FFKonv	Form factor of the convex contour
Loch	Relative proportion of nuclear holes
nGran	Number of coarse chromatin particles
MaxTextK	Number of relative maxima of the texture curve
IODnc	Integrated optical density without correction for section thickness
RIODHet	Ratio of heterochromatin and IOD
FS1M	Mean extinction of the “flat image” (first moment of fine structure)
FS2M	Standard deviation of the extinction of the “flat image” (second moment of fine structure)
FS3M	Skewness of the extinction of the “flat image” (third moment of the fine structure)
IOD	Integrated optical density
Rad STD	Relative standard deviation of the radial extinction
InvMo	52 invariant moments of heterochromatin according to Hu
FnGran-FFS3M	Features nGran-FFS3M in a median filtered image
Node	Number of nodes in the texture tree
Width	Width of the texture tree

Table 4
Flow chart of analyses

Flow chart of analyses
Localisation of 500 cells per case and coding of the immunohistochemical staining
Destaining during a 45 min 5N HCl hydrolysis
Feulgen staining
Relocalisation of the coded nuclei
Cytometric measurement (63× objective, oil immersion)
Computing of 97 nuclear features, describing the size, shape, chromatin topology and distribution
Multivariate statistical analyses

3. Results

3.1. Nuclear morphology of tumours with a different p53 expression

In this part, only the immunoreactive score of the whole tumour will be taken into consideration. All nuclei independent of their individual p53 status were pooled for each case.

There were significant differences in differently scored tumours in most prognostic subgroups. In the subgroups pT2–4, pN0 and pN1–2 an increasing immunoreactive score was associated with a higher variability in the shape of the nuclei. Some features describing the amount and the distribution of chromatin showed significant differences within each subgroup of tumours.

The analysis of cancers in groups with favourable (pT1pN0) and unfavourable prognostic (pT2–4pN1–2) stages could not demonstrate any morphological differences between the differently scored p53 status (Table 5; Figs 1 and 2).

Features of the size or the shape of the nuclei did not play any role in the tumour groups with the Bloom–Richardson grade two or three. In these categories the features of chromatin distribution only showed significant differences.

3.2. Nuclear morphology of p53 subpopulations within clinicopathological subgroups

Differences were found in the nuclear morphology between cells showing differences in their p53 expression in the most groups with specific clinicopathological features.

Table 5
Tumours with different p53 expression in clinicopathological subgroups

p53-IRS	0	1–4	5–12	F	$p\%^*$
pT2–4					
S.D. FormFak	1.7955	2.1467	2.2413		
S.D. IODnc	7003.3	8431.9	11402		
S.D. FRIODHet	0.15122	0.18093	0.16986	17.42	$<$0.0001
pN0					
FMaxTextK	5.7217	3.7576	5.4886		
S.D. FFKonv	0.90175	0.85447	1.0158		
S.D. IODnc	7406.4	6883.4	11740		
S.D. RadSTD	0.032723	0.027417	0.03136	12.95	0.009
pN1–2					
IOD	50979	48930	55281		
S.D. FormFak	1.6370	2.1082	2.2077		
S.D. IODnc	6736.1	8007.7	12129	13.58	0.005
BR2					
nGran	35.458	37.190	39.693		
S.D. Node	5.1816	6.0881	7.2236		
S.D. Width	2.5324	2.9739	3.4221	38.24	$<$0.0001
BR3					
FRIODHet	0.28286	0.41516	0.43772	8.74	0.094

IRS 0 . . . p53 negative tumours; IRS 1–4 . . . weakly p53 positive tumours; IRS 5–12 . . . strongly p53 positive tumours.

*Considering the Bonferroni criterion the significance level for the multivariate discrimination between the groups is set at $p = 0.1$.

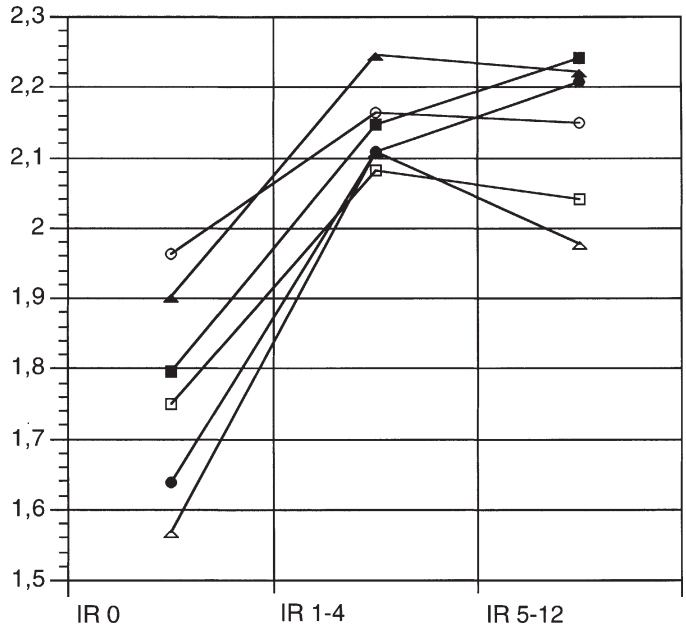

Fig. 1. Standard deviation of the shape factor (S.D. FormFak) in breast cancers with different p53 expression in correlation to the tumour size and the lymph node status.
IR 0 . . . p53 negative tumours; IR 1–4 . . . weakly p53 positive tumours; IR 5–12 . . . strongly p53 positive tumours. □ pT1; ■ pT2–4; ○ pN0; ● pN1–2; △ pT1pN0; ▲ pT2–4pN1–2.

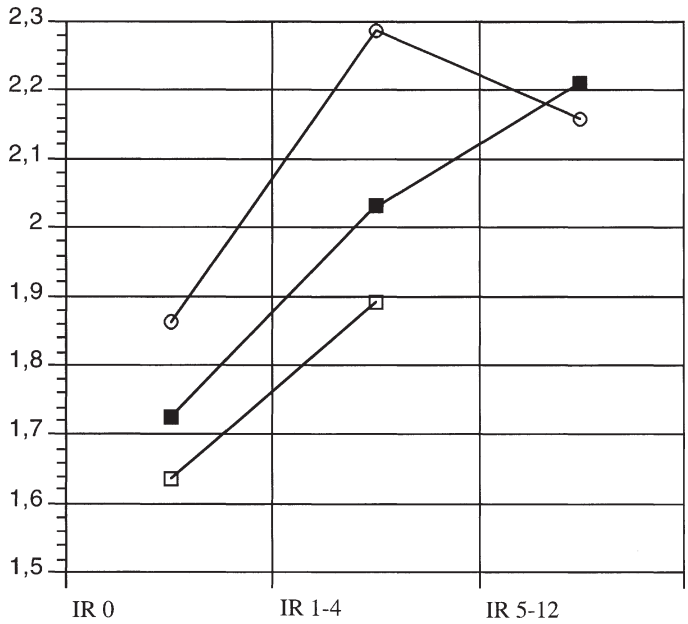

Fig. 2. Standard deviation of the shape factor (S.D. FormFak) in breast cancers with different p53 expression in correlation to the Bloom–Richardson grading.
IR 0 . . . p53 negative tumours; IR 1–4 . . . weakly p53 positive tumours; IR 5–12 . . . strongly p53 positive tumours. □ G1*; ■ G2; ○ G3.
*Excluded from statistical analysis, the number of cases was too small for statistical analysis.

Table 6
Nuclei with different p53 expression in p53 positive tumours in prognostic subgroups

p53	−	+	++	+++	F	$p\%^*$
pT1						
invMo17	0.1874×10^{-5}	0.2761×10^{-5}	0.4594×10^{-5}	0.8943×10^{-5}		
S.D. FS3M	1.2077	1.2448	1.4833	2.0073		
S.D. IOD	14691	17165	21568	42083	11.82	0.001
pT2						
FExtGran	1.2885	1.2769	1.2602	1.2356		
S.D. IOD	14643	19592	21706	28877	15.14	<0.0001
pN0						
S.D. IODnc	6996.6	7656.9	10838	15494	6.13	0.112
pN1–2						
FExtGran	1.2738	1.2737	1.2593	1.2315		
S.D. IOD	15122	20711	21870	28414	18.4	<0.0001
BR2						
FFKonv	13.629	13.788	13.976	14.175		
S.D. IODnc	7474.2	7881.1	11118	13521	11.84	0.001
BR3						
FRIODHet	0.39745	0.41164	0.46287	0.54492	6.28	0.085
pT1pN0						
S.D. InvMo41	0.60514×10^{-5}	0.36111×10^{-5}	0.18669×10^{-4}	0.18324×10^{-3}	10.41	0.006
pT2–4pN1–2						
FExtGran	1.2882	1.2759	1.2571	1.2320		
S.D. FS1M	0.10655	0.090770	0.088173	0.084649		
S.D. IOD	17264	21064	22780	27752	10.92	0.001

S.D. . . . standard deviation; $-$ . . . p53 negative nuclei; $+$ . . . weakly p53 positive nuclei; $++$ . . . moderately p53 positive nuclei; $+++$ . . . strongly p53 positive nuclei.
*Considering the Bonferroni criteria the significance level for the multivariate discrimination between the groups is set at $p = 0.1$.

As shown in Table 6, within the subgroups of different tumour sizes (pT1, pT2) or different lymph node status (pN0, pN1–2) the standard deviation of the IOD increases with a higher p53 stainability. Other features with significant differences in some groups describe the distribution and topography of the chromatin.

In small breast cancers without lymph node metastases (pT1pN0) the statistical analysis demonstrated the standard deviation of an invariant moment to be inversely correlated to the p53 expression, whereas in tumours with unfavourable prognostic criteria (pT2–4pN1–2) differences in two features of the chromatin distribution and the standard deviation of the IOD were found (Fig. 3).

The nuclear populations with different p53 expression in tumours with the same degree of malignancy were different with respect to their chromatin distribution. Only the tumours with a Bloom–Richardson grade two showed a more irregular shape of the strong p53 positive nuclei compared with their weaker positive or negative counterparts (Table 6; Fig. 4).

However, if the p53 positive nuclei or the p53 negative nuclei were compared within the subgroups with the same tumour size, lymph node status, or Bloom–Richardson grade no differences could be found in the nuclear morphology.

3.3. Comparison of clinicopathological subgroups with positive or negative p53 stage

Taking into consideration the p53 immunoreactivity of the pooled cells of each tumour, few differences in the nuclear structure between the clinicopathological defined tumour subgroups were found.

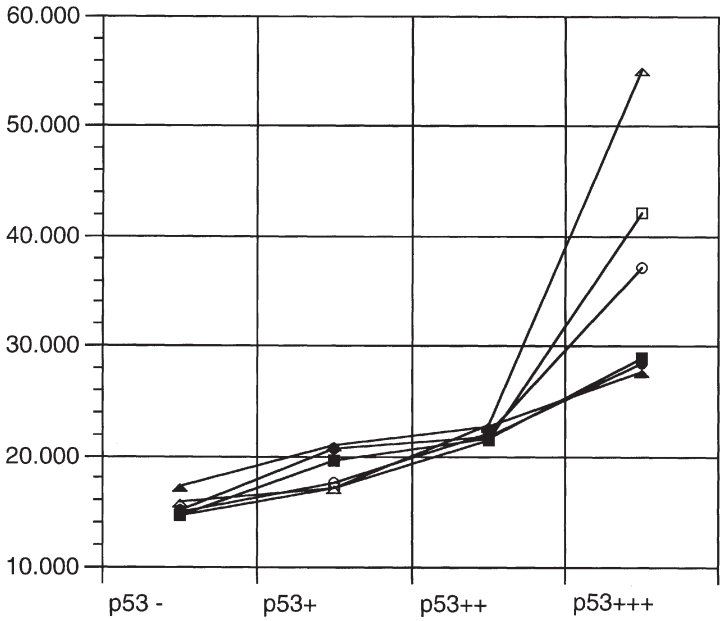

Fig. 3. Standard deviation of integrated optical density (S.D. IOD) in nuclear populations with different p53 expression in correlation to the tumour size and the lymph node status.
p53− . . . p53 negative nuclei; p53+. . . weakly positive nuclei; p53++. . . moderately positive nuclei; p53+++. . . strongly positive nuclei. □ pT1; ■ pT2–4; ○ pN0; ● pN1–2; △ pT1pN0; ▲ pT2–4pN1–2.

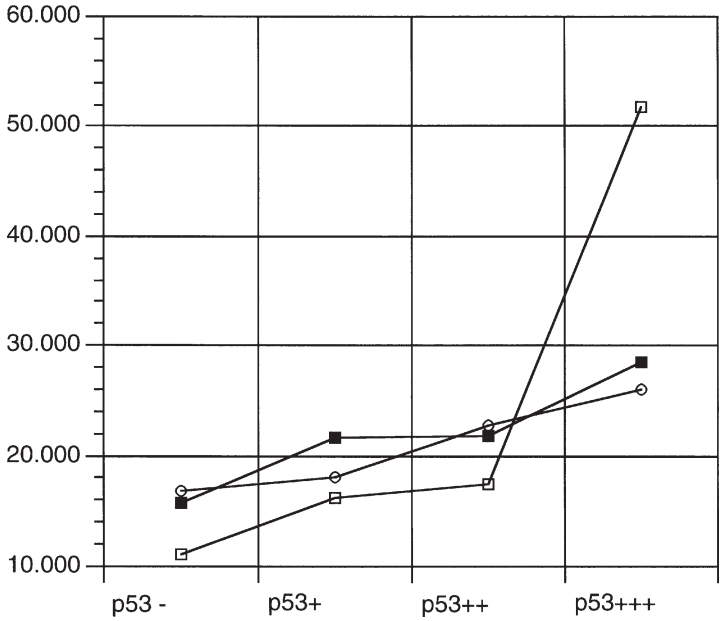

Fig. 4. Standard deviation of integrated optical density (S.D. IOD) in nuclear populations with different p53 expression in correlation to the Bloom–Richardson grading.
p53− . . . p53 negative nuclei; p53+ . . . weakly positive nuclei; p53++. . . moderately positive nuclei; p53+++ . . . strongly positive nuclei. □ G1*; ■ G2; ○ G3.
*Excluded from statistical analysis, the number of cases was too small for statistical analysis.

Table 7
p53 positive tumours with and without lymph node metastases

pT2–4	pN0	pN1–2	F	$p\%^*$
FormFak	18.496	18.763		
FFS2MpM	0.28186	0.21335	36.31	0.001

*Considering the Bonferroni criteria the significance level for the multivariate discrimination between the groups is set at $p = 0.1$.

Table 8
p53 negative cases. Comparison of different clinicopathological features

BR grade	BR1	BR2	BR3	F	$p\%$
Width	6.2201	7.8594	10.527	7.94	0.163

pT1	pN0	pN1–2	F	$p\%$
RVKonv	0.73273	0.69923		
S.D. Loch	0.046191	0.064795		
S.D. InvMo24	0.16968×10^{-2}	0.26044×10^{-2}		
S.D. InvMo41	0.38177×10^{-3}	0.87135×10^{-3}	47.02	0.002

p53 positive breast cancers with a diameter greater than 2 cm differed in a shape feature and a feature of the fine structure when node negative and node positive tumours were compared (Table 7).

In the p53 negative breast cancers with a tumour size smaller than 2 cm, the node negative tumours were also different from the cancers with lymph node metastases in the nuclear shape and the chromatin distribution. Additionally, there were differences in invariant moments. The mean value of the feature width of texture tree increases with the grade of malignancy in the p53 negative tumours (Table 8).

4. Discussion

The immunohistochemical detection of the p53 gene product can be regarded as a sign of the mutation of this tumour suppressor gene [27]. The mutation of the p53 may be associated with a loss or change of its function, resulting in a higher genetic instability. The changes in the genome of a tumour determine the biological properties of the tumour and its clinical behaviour, which is reflected in the tumour size, occurrence of metastases or grade of differentiation.

Correlations between an unfavourable prognosis and the immunohistochemical detection of the p53 protein were also found in other breast cancers [7–9,11,12,16,17,21,29,31,32]. In a previous study, we found that there were differences in the morphology of the nuclei in the p53 expression by means of TV based image cytometry [18].

The disturbance of the p53 function may influence the nuclear morphology in several ways. The p53 mutation itself may lead to changes in the DNA conformation, for example by a change of the tertiary structure or by an altered binding to histone proteins. The loss of the control function of p53 in the cell cycle can result in a higher number of proliferating cells, caused by an unhindered G1-S-transition. The process of proliferation is associated with changes in the DNA conformation, which occurred in a higher part of the p53 positive tumours. The loss of the control function also allows the transmission of other genetic defects, resulting in further aberrations of the nuclear structure.

The aim of this study was to investigate changes in the nuclear structure depending on the p53 expression in breast cancers with special clinicopathological characteristics, also displaying different stages of the tumour progression. Furthermore, the possible association of specific nuclear patterns

with the p53 expression in some tumour groups and the role of p53 negative and p53 positive nuclear populations for the nuclear morphology in prognostic subgroups were points of interest. In most clinicopathological subgroups we found differences in the nuclear morphology dependent on the p53 immunostaining both between the nuclear populations and the differently scored tumours.

If the immunoreactive score of the pooled cells of the whole tumour was taken into consideration, the standard deviations of shape features increased with the immunoreactive score in all clinicopathological subgroups except the groups characterised by the Bloom–Richardson grade. The absence of significant differences in shape features in tumours with the same degree of differentiation may be due to the evaluation of the nuclear pleomorphism as a criterion in the grading system.

The comparison of differently scored cases also demonstrated a non-uniform tendency in some features. The cases with a score 1–4 showed partly lower or higher values than their negative or stronger positive counterparts. This may be caused by the immunohistochemical detection of the p53 gene product. The antibody DO-1 recognises an epitope which exists in the mutated protein as well as in the p53 wild type protein. It is possible that the life time of the wild type protein may be also prolonged and can be detected by immunohistochemistry. The reaction could be weak in such tumours. Once again, not all mutations of the p53 gene necessarily lead to a immunohistochemically defined detectable phenotype; a small number of the p53 negative tumours could also contain cells with a mutated p53 gene.

In comparison with the nuclear populations, features describing the chromatin distribution and/or amount were different in most prognostic subgroups. A higher degree of irregularity in the nuclear shape in the stronger p53 positive nuclei than in the negative or weakly positive nuclei was found only in breast cancers with a Bloom–Richardson grade two.

The morphological heterogeneity between nuclei with different p53 expression was higher in tumours with favourable prognostic criteria than in tumours with poor prognosis (see Table 4 and Figs 3 and 4). The nuclear morphology of tumours with poor prognosis should reflect a higher degree of dedifferentiation, which is influenced by many factors and should also contain the p53 negative nuclei. In cancers with a favourable prognosis, the higher variability of nuclear morphologic features concerning the p53 expression may give a hint of the role of the p53 mutation in the process of tumour progression. The loss of the repair function of p53 protein results in a genetic instability, which is followed by an accelerated tumour progression.

Significant differences in the standard deviation of the IOD, describing the well-known phenomenon of the polychromasia in malignancies, were shown in many subgroups of tumours in association with the p53 status. Therefore, the correlation between p53 expression, nuclear morphology and the ploidy should be a topic of ongoing studies.

In another study, we examined breast cancer cells with different progesterone receptor (PgR) expression with the same method used in this study on the p53 expression. The stronger PgR positive nuclei are smaller and showed a lower degree of granularity than their negative or weakly positive counterparts. In general, the nuclei with a positive PgR reaction displayed a morphology that is assumed to be linked with a better prognosis [18].

Other authors also reported a morphological heterogeneity of the nuclei in correlation to functional parameters of the cells. For example, there are studies on the changes in the nuclear features in chemoresistent or chemosensitive tumours or changes during the cell culture [10,13,28]. Larsimont et al. [26] found by means of image analysis and a conventional biochemical assay for the oestrogen receptor a more dispersed chromatin and smaller nuclei in breast cancer with a higher receptor content than in the tumours with a low oestrogen receptor content or without oestrogen receptors.

In a methodological approach similar to that presented in this paper, Falkmer et al. [14,15] was able to show differences in the DNA content of tumour cells with different expression of neuroendocrine markers.

The analysis without taking the p53 expression into consideration showed only significant differences in the nuclear image in correlation with the Bloom–Richardson grading (data not shown). One of the possible reasons for this is the small number of cases in this study. In spite of this fact the cases were selected by their p53 status and not by a random or a consecutive sampling as in the above mentioned studies. In some other studies especially the shape and the size of nuclei played a role in correlation with the lymph node status [2]. Aubele et al. [2] demonstrated the value of the shape and texture features for the prognosis in a group of more than 500 node negative breast cancer.

Theissig et al. [38] found differences in the chromatin structure between prognostic groups of breast cancers.

In conclusion, the results demonstrate the relationship between the nuclear morphology by the method of high resolution image analysis, and a functional state of cells: in this study the p53 expression. The study showed that the population of p53 negative or p53 positive nuclei alone does not influence the nuclear features in comparison with clinicopathological categories. The immunohistochemical detectable p53 protein plays a role in the progression of a malignant tumour, but this is not the only one. Especially in tumours with an unfavourable prognosis, the p53 status is not the only parameter that determines the nuclear morphology and the clinicopathological features.

Acknowledgements

We thank Dr Vojtesek for the kind gift of the antibody DO-1. We are grateful to Mrs Langer, Mrs Konrad and Mrs Riester for excellent technical assistance.

References

[1] C.G. Allred, G.M. Clark, R. Elledge, S.A.W. Fuqua, R.W. Brown, G.C. Chamness, C.K. Osborne and W.L. McGuire, Association of p53 protein expression with tumor cell proliferation rate and clinical outcome in node-negative breast cancer, *J. Natl. Cancer Inst.* **85** (1993), 200–206.

[2] M. Aubele, G. Auer, A. Voss, U. Falkmer, L.-E. Ruitquist and H. Höfler, Different risk groups in node negative breast cancer: Prognostic value of cytophotometrically assessed DNA, morphometry and texture, *Int. J. Cancer* **63** (1995), 7–12.

[3] G.U. Auer, R.G. Steinbeck and A.D. Zetterberg, Molecular markers in diagnostic pathology, Compendium on the Computerized Cytology and Histology Laboratory, 1994, 129–142.

[4] D.M. Barnes, E.A. Dublin, C.J. Fisher, D.A. Levison and R.R. Millis, Immunohistochemical detection of p53 protein in Mammary carcinoma: An important new independent indicator of prognosis?, *Hum. Pathol.* **24** (1993), 469–476.

[5] H. Battifora, ed., p53 Immunohistochemistry: A word of caution, *Hum. Pathol.* **25** (1994), 435–437.

[6] H.J.G. Bloom and W.W. Richardson, Histologic grading and prognosis in breast cancer, *Br. J. Cancer.* **11** (1957), 359–377.

[7] G. Cattoretti, F. Rilke, S. Andreola, L. D'Amato and D. Delia, p53 expression in breast cancer, *Int. J. Cancer* **41** (1988), 178–183.

[8] K. Chang, I. Ding, F.G. Kern and M.C. Willingham, Immunohistochemical analysis of p53 and HER- 2/neu proteins in human tumors, *J. Histochem. Cytochem.* **39** (1991), 1281–1287.

[9] C. Charpin, B. DeVictor, L. Andrac, J. Amabile, D. Bergert, M.-N. LaVaut, C. Allasia and L. Piana, p53 quantitative immunocytochemical analysis in breast cancer, *Hum. Pathol.* **26** (1995), 159–166.

[10] E. Colomb, C. Dussert and P.-M. Martin, Nuclear texture parameters as discriminant factors in cell cycle and drug sensitive studies, *Cytometry* **12** (1991), 15–25.

[11] A.M. Davidoff, J.E. Herndon, N.S. Glover, B.-J.M. Kerns, J.C. Pence, J.D. Iglehart and J.R. Marks, Relation between p53 overexpression and established prognostic factors in breast cancer, *Surgery* **110** (1991), 259–264.
[12] W. Domagala, B. Harezga, A. Szadowska, M. Markiewski, K. Weber and M. Osborn, Nuclear p53 protein accumulates preferentially in medullary and high-grade ductal but rarely in lobular breast carcinomas, *Am. J. Pathol.* **142** (1993), 669–674.
[13] J. Dufer, C. Millot-Broglio, Z.O. Hamed, F. Liautaud-Roger, P. Joly, A. Desplaces and J.-C. Jardillier, Nuclear DNA content and chromatin texture in multidrug-resistant human leukemic cell lines, *Int. J. Cancer* **60** (1995), 108–114.
[14] U.G. Falkmer and S. Falkmer, The value of cytometric DNA analysis as a prognostic tool in neuroendocrine neoplastic diseases, *Path. Res. Pract.* **191** (1995), 251–303.
[15] U.G. Falkmer, A. Höög, H. Schimmelpfennig, O. Ahrens, G. Auer and S. Falkmer, A technique for cytometric DNA assessments of the nuclei of immunohistochemically identified neuroendocrine parenchymal cells, *Cytometry* **12** (1991), 26.
[16] K. Friedrich, V. Dimmer, G. Haroske, A. Loßnitzer, M. Kasper, F. Theissig and K.D. Kunze, Expression of p53 and bcl-2 in correlation to clinicopathological parameters, hormone receptor status and DNA ploidy in breast cancers, *Path. Res. Pract.* **191** (1995), 1114–1121.
[17] W. Gorczyca, M. Markiewski, A. Kram, T. Tuziak and W. Domagala, Immunohistochemical analysis of bcl-2 and p53 expression in breast carcinomas: their correlation with Ki-67 growth fraction, *Virchows Archiv* **426** (1995), 229–233.
[18] G. Haroske, V. Dimmer, K. Friedrich, W. Meyer, B. Thieme, F. Theissig and K.D. Kunze, Nuclear image analysis of immunohistochemically stained cells in breast carcinomas, *Histochem. Cell Biol.* **105** (1996), 479–485.
[19] G. Haroske, K. Friedrich, F. Theissig, W. Meyer and K.D. Kunze, Heterogeneity of the chromatin fine structure in DNA-diploid breast cancer cells, *Anal. Cell. Pathol.* **8** (1995), 213–226.
[20] G. Haroske, W.D. Meyer, F. Theissig and K.D. Kunze, Increase of precision and accuracy of DNA cytometry by correcting diffraction and glare errors, *Anal. Cell. Pathol.* **9** (1994), 1–12.
[21] J. Hurlimann, Prognostic value of p53 protein expression in breast carcinomas, *Path. Res. Pract.* **189** (1993), 996–1003.
[22] *International Histological Classification of Tumors. Histological Typing of Breast Tumours*, 2nd ed., WHO, Geneva, 1981.
[23] M.B. Kastan, O. Onyekwere, D. Sidransky, B. Vogelstein and R.W. Craig, Participation of p53 protein in the cellular response to DNA damage, *Cancer Res.* **51** (1991), 6304–6311.
[24] K.D. Kunze, G. Haroske, V. Dimmer, W. Meyer and F. Theissig, Grading and prognosis of ductale mammary carcinoma by nuclear image analysis in tissue sections, *Path. Res. Pract.* **185** (1989), 689–693.
[25] D.P. Lane, p53, guardian of the genome, *Nature* **358** (1992), 15–16.
[26] D. Larsimont, R. Kiss, D. d'Olne, Y. de Launoit, W. Mattheiem, R. Paridaens, J.-L. Pasteels and C. Gompel, Correlation between nuclear cytomorphometric parameters and estrogen receptor levels in breast cancer, *Cancer* **63** (1989), 2162–2168.
[27] A.J. Levine, J. Momand and C.A. Finlay, The p53 tumour suppressor gene, *Nature* **351** (1991), 453–456.
[28] B.-M.E. Ljung, D.H. Moore, F.M. Waldman, K.L. Chew, B.H. Mayall and H.S. Smith, Effects of short-term culture on benign and malignant human breast epithelium analyzed by image analysis, *Anal. Quant. Cytol. Histol.* **15** (1993), 107–114.
[29] P. Lipponen, H. Ji, S. Aaltomaa, S. Syrjänen and K. Syrjänen, p53 protein expression in breast cancer as related to histopathological characteristics and prognosis, *Int. J. Cancer* **55** (1993), 51–56.
[30] G.M. Mariuzzi, V. Mambelli, P. Criante and S. Sisti, Quantitative evaluation of morphological parameters for infiltrating ductal breast cancer prognosis, *Path. Res. Pract.* **185** (1989), 698–700.
[31] M. Martinazzi, Expression of p53 oncoprotein in different histological types of breast carcinoma, *Am. J. Pathol.* **144** (1994), 205.
[32] J.L. Ostrowski, A. Sawan, L. Henry, C. Wright, C. Hennessy, T.J.W. Lennard, B. Agnus and C.H.W. Horne, p53 expression in human breast cancer related to survival and prognostic factors: an immunohistochemical study, *J. Pathol.* **164** (1991), 75–81.
[33] O. Pauwels and R. Kiss, Computerized morphonuclear analyses of Feulgen-stained nuclei from 11 chemosensitive and from 11 chemoresistant neoplastic cell lines, *Anal. Cell. Pathol.* **7** (1994), 235–250.
[34] P.L. Porter, A.M. Gown, S.G. Kramp and M.D. Coltrera, Widespread p53 overexpression in human malignant tumors, *Am. J. Pathol.* **140** (1992), 145–153.
[35] W. Remmele and H.E. Stegner, Vorschlag zur einheitlichen Definition eines immunreaktiven Score (IRS) für den immunohistochemischen Estrogenrezeptor-Nachweis (ER-IRA) im Mammakarzinomgewebe, *Pathologe* **8** (1987), 138–140.
[36] R. Silvestrini, E. Benini, M.G. Daidone, S. Veneroni, P. Borachi, V. Cappelletti, G. di Fronzo and U. Veronesi, p53 as an independent prognostic marker in lymph node-negative breast cancer patients, *J. Natl. Cancer Inst.* **85** (1993), 965–970.

[37] B. Stenkvist, E. Bengtsson, O. Erikson, T. Jarkrans and B. Nordin, Image cytometry in malignancy grading of breast cancer. Results in a prospective study with seven years of follow-up, *Analyt. Quant. Cytol. Histol.* **4** (1986), 293–300.
[38] F. Theissig, V. Dimmer, G. Haroske, K.D. Kunze and W. Meyer, Use of nuclear image cytometry, histopathological grading and DNA cytometry to make breast cancer prognosis more objective, *Anal. Cell. Pathol.* **3** (1991), 351–360.
[39] B. Vojtesek, J. Bartek, C.A. Midgley and D.P. Lane, An immunochemical analysis of the human nuclear phosphoprotein p53. New monoclonal antibodies and epitope mapping using recombinant p53, *J. Immunol. Meth.* **151** (1992), 237–244.